

# UC San Diego

## UC San Diego Previously Published Works

### Title

Rates of Choroidal Microvasculature Dropout and Retinal Nerve Fiber Layer Changes in Glaucoma

### Permalink

<https://escholarship.org/uc/item/5w40t48f>

### Authors

Micheletti, Eleonora  
Moghimi, Sasan  
Nishida, Takashi  
et al.

### Publication Date

2022-09-01

### DOI

10.1016/j.ajo.2022.04.024

Peer reviewed



Published in final edited form as:

*Am J Ophthalmol.* 2022 September ; 241: 130–138. doi:10.1016/j.ajo.2022.04.024.

## Rates of Choroidal Microvasculature Dropout and Retinal Nerve Fiber Layer Changes in Glaucoma

Eleonora Micheletti<sup>1,\*</sup>, Sasan Moghimi<sup>1,\*</sup>, Takashi Nishida<sup>1</sup>, Nevin El-Nimri<sup>1</sup>, Golnoush Mahmoudinezhad<sup>1</sup>, Alireza Kamalipour<sup>1</sup>, Harsha L. Rao<sup>3,4</sup>, Linda M. Zangwill<sup>1</sup>, Robert N. Weinreb<sup>1</sup>

<sup>1</sup>Hamilton Glaucoma Center, Shiley Eye Institute, Viterbi Family Department of Ophthalmology, University of California San Diego, La Jolla, California

<sup>3</sup>Narayana Nethralaya, Bangalore, India.

<sup>4</sup>University Eye Clinic Maastricht, University Medical Center, Maastricht, the Netherlands.

### Abstract

**Purpose:** To evaluate the association between rates of choroidal microvasculature dropout (MvD) change and rates of circumpapillary retinal nerve fiber layer (cpRNFL) loss in primary open-angle glaucoma (POAG) eyes.

**Design:** Cohort study from clinical trial data

**Methods:** A total of 91 eyes of 68 POAG patients with and without localized MvD at baseline with at least 4 visits and 2 years follow-up with optical coherence tomography angiography (OCT-A) and OCT scans were included. Area and angular circumference of MvD were evaluated on OCT-A en-face and B-scan choroidal vessel density images during the follow-up period. Joint longitudinal mixed effects models were used to estimate the rates of change in MvD area or angular circumference and RNFL thickness. Univariable and multivariable regressions were completed to identify the factors contributing to cpRNFL thinning.

**Results:** MvD was identified in 53 (58.2%) eyes at baseline. Seventeen eyes (18.6%) eyes that did not show MvD at baseline developed it over the follow-up period. Over a mean follow-up of 4.0 years, the mean rates of change of MvD area and angular circumference (95%CI) were 0.05 (0.04, 0.06) mm<sup>2</sup>/year, and 13.2 (10.7, 15.8) degree/year, respectively. In multivariable models, the rate of cpRNFL thinning was significantly associated with the rates of change of MvD area and angular circumference (P=0.008 and P=0.009, respectively).

**Conclusions:** Rates of MvD area and angular circumference change over time were associated with concurrent rates of cpRNFL loss in POAG eyes.

### Table of Contents Statement – AJO-22–102

**Corresponding Author:** Robert N. Weinreb, MD, Shiley Eye Institute, University of California, San Diego, 9500 Campus Point Drive, La Jolla, CA, 92093-0946, rweinreb@ucsd.edu, +1(858) 534-6290.

\*These authors had equal contributions as co-first authors.

#### AUTHOR CONTRIBUTION

Concept design: EM, SM, RNW; Acquisition and reviewing data: TN, SM, NEN, TN, GM, AK; Analysis or interpretation of data: EM, SM, TN, GM, HLR, LMZ, RNW; Drafting of the manuscript: EM, SM, TN, HLR, RNW; Critical revision of the manuscript: All authors; Obtained funding: SM, LMZ, RNW; Supervision: SM, HLR, LMZ, RNW

Faster change in Choroidal Microvasculature Dropout area and angular circumference was moderately, and significantly, associated with faster concurrent Retinal Nerve Fiber Layer loss in a cohort of Open-Angle Glaucoma patients during a mean follow-up of four years.

## Keywords

Choroidal Microvasculature Dropout change; retinal nerve fiber layer thinning; optical coherence tomography angiography; glaucoma progression

## INTRODUCTION

Glaucoma is a progressive optic neuropathy characterized by structural changes in the optic nerve head (ONH), circumpapillary retinal nerve fiber layer (cpRNFL) and accompanying damage in the visual field (VF).<sup>1,2</sup> Although the pathophysiological process in glaucoma is still unclear, the vascular system and, in particular, the retinal and choroidal microvasculature, seem to have a contributory role.<sup>3,4</sup>

A localized parapapillary perfusion defect, known as choroidal microvasculature dropout (MvD), has been well recognized in the choroidal layer of glaucoma patients on optical coherence tomography angiography (OCT-A) scans. MvD was found to correspond to perfusion defects on indocyanine green angiography<sup>5</sup>, indicating that MvD represents a true circulatory defect in the peripapillary choroid related to a compromised perfusion in the deep tissues of the optic nerve head (ONH).<sup>5,6</sup> When detected at baseline, MvD was associated with progressive VF loss and/or cpRNFL thinning.<sup>7-9</sup> Moreover, its area topographically corresponded with the location of cpRNFL defects in the majority of the eyes.<sup>10,11</sup> Recently, an enlargement of peripapillary MvD was observed in glaucomatous eyes and these changes in size appeared to be greater in eyes with accelerated glaucoma progression.<sup>12</sup>

Disc hemorrhage (DH)<sup>13-15</sup> and decreased ocular perfusion pressure<sup>16</sup> have been strongly associated with the presence of MvD. Other studies reported a topographic association between MvD and LC defects<sup>6,17,18</sup>. This suggests that a microvasculature impairment involving LC and peripapillary choroid, both supplied by the short posterior ciliary artery, may explain the structural changes of the LC and lead to MvD.<sup>19</sup> Localized perfusion defects in the peripapillary choroid have been more frequently seen in eyes with initial parafoveal VF defects within a 10° radius compared to eyes with initial nasal VF damage.<sup>14</sup> In addition, systemic risk factors, such as diastolic blood pressure, cold extremities, migraine, known to be associated with parafoveal scotomas<sup>20</sup>, have been associated with MvD.<sup>6,21</sup> These findings suggest that the presence of MvD may be part of a specific pattern of glaucomatous central VF loss with an underlying pathogenetic mechanism of glaucomatous optic neuropathy. The loss of sensitivity in the central area of the VF carries a greater impact on the ability to perform activities of daily living in patients diagnosed with glaucoma. Therefore, its progressive decline is closely related to faster decline in quality of life of glaucoma patients.<sup>22</sup>

The current study aims to evaluate whether changes of MvD over time is related to progressive cpRNFL thinning. This may enhance our understanding of the role of MvD in the glaucoma monitoring and provide a rationale for utilizing MvD changes as a potential marker of glaucoma progression.

## METHODS

This longitudinal study included POAG patients enrolled in Diagnostic Innovations in Glaucoma Study (DIGS)<sup>23,24</sup> who underwent OCT-A (Angiovue; Optovue Inc., Fremont, CA) and spectral-domain OCT (Spectralis, Heidelberg Engineering, Germany) imaging. Participants were assessed longitudinally according to a standard protocol consisting of regular follow-up visits with clinical examination, imaging, and functional tests. All participants from the DIGS study who met the inclusion criteria described below were included. Informed consent was obtained from all study participants. The University of California, San Diego Human Subject Committee approved all protocols, and the methods described adhered to tenets of the Declaration of Helsinki.

This study included eyes with a minimum of 4 qualified OCT-A and OCT scans of ONH and a minimum of 2 years follow-up. Eyes were classified as glaucoma if they had repeatable (at least 2 consecutive) abnormal VF test results with evidence of glaucomatous optic neuropathy – defined as excavation, the presence of focal thinning, notching of neuroretinal rim, or localized or diffuse atrophy of the cpRNFL on the basis of masked grading of optic disc photographs by 2 graders. An abnormal VF test was defined as a pattern standard deviation ( $P < 0.05$ ) or a Glaucoma Hemifield Test result outside normal limits.

Inclusion criteria also included (1) older than 18 years of age, (2) open angles on gonioscopy, and (3) best-corrected visual acuity of 20/40 or better at study entry. Exclusion criteria were (1) history of trauma or intraocular surgery (except for uncomplicated cataract surgery or glaucoma surgery), (2) coexisting retinal disease, (3) uveitis, (4) non-glaucomatous optic neuropathy, and (5) axial length of 27 mm or more. Participants with the diagnosis of systemic diseases such as Parkinson's disease, Alzheimer's disease, dementia, or a history of stroke were excluded. Those with poor-quality OCTA and OCT were also excluded.

### OCT Measurements

The Spectralis SDOCT (Spectralis HRA+OCT, software version 5.4.7.0; Heidelberg Engineering, Inc.) was used for cpRNFL thickness measurements. The details of the SDOCT imaging have been previously reported.<sup>25</sup> The cpRNFL thickness was measured using a high-resolution cpRNFL circle scan consisting of 1536 A-scan points from a 3.45mm circle centered on the optic disc. Follow-up scans were performed using a built-in automated realignment procedure (referred to as the follow-up examination in the system documentation). The accuracy of the segmentation of the cpRNFL was reviewed and segmentation errors were fixed manually by Imaging Data Evaluation and Analysis Reading (IDEA) Center personnel.

### Choroidal microvasculature dropout detection

ONH 4.5 X 4.5 mm<sup>2</sup> (304 B-scans x 304 A-scans per B-scan) centered on the ONH were acquired with the AngioVue OCT-A system (software version 2018.1.1.63). The retinal layers of each scan were segmented automatically by the AngioVue software and the en-face choroidal vessel density map was acquired. Only good-quality images were included. OCT-A and SD-OCT image quality review was completed according to the IDEA Center standard protocol on all scans processed with standard AngioVue software. Poor-quality images were excluded; these were defined as images with 1) low scan quality with quality index (QI) of less than 4; 2) poor clarity; 3) residual motion artifacts visible as irregular vessel pattern or disc boundary on the en-face angiogram; 4) image cropping or local weak signal resulting from vitreous opacity; or 5) segmentation errors that could not be corrected. Dropout was required to be present in at least 4 consecutive horizontal B-scans and also to be >200 µm in diameter in at least one scan and to be in contact with the OCT disc boundary. The optic disc boundary was automatically detected by the Optovue software. In case of errors in disc demarcation, one trained observer masked to the clinical information of the subjects corrected the disc boundary manually by searching for the position of Bruch's membrane opening (BMO), as previously described.<sup>26</sup> Two observers, who were masked to the clinical characteristics of the participants independently determined the presence or absence of MvD for each patient.

### Assessment of MvD area, circumferential angle and location

Optic disc and the peripapillary atrophy (PPA) margins were detected by simultaneously viewing the stereoscopic optic disc photographs and the scanning laser ophthalmoscopic (SLO) images that were obtained along with the OCT-A images. MvD area was manually demarcated on en-face choroidal vessel density maps using the line tool provided by ImageJ software (Version 1.53; available at <http://imagej.nih.gov/ij/download.html>; *National Institute of Health, Bethesda, Maryland, USA*). Littmann's formula was used to correct the ocular magnification in OCT-A.<sup>27,28</sup> Details of the formula are provided elsewhere.<sup>28</sup> The Avanti SD OCT has a default axial length of 23.95 mm and an anterior corneal curvature radius of 7.77 mm.

MvD angular circumference was measured as previously described.<sup>12</sup> In brief, the two points at which the extreme borders of MvD area met the ONH border were identified and defined as angular circumferential margins. The angular circumference was then determined by drawing two lines connecting the ONH center to the angular circumference margins of the MvD.

Both area and angular circumference of the MvD were assessed by two trained graders who were masked to the clinical data of the patients, including cpRNFL data (EM and NEN). Any uncertainty was resolved by a glaucoma specialist, designated as the third grader (SM). MvD area that included large retinal vessels was included as part of the MvD area if the MvD extended beyond the vessels. In cases where the retinal vessels were located at the border of the MvD, the area covered by the vessels was excluded from the MvD area. Reflectance or shadowing of the large vessels on the horizontal and en-face images was excluded from the quantitative analysis by the two independent graders. In an eye showing

more than one MvD, the area and the angular extent of each MvD were calculated separately and then added together to determine the total area and the total angular extension of MvD for the eye.

The sectoral location of the dropout was determined based on the 8 separate sectors corresponding to those on the cpRNFL vessel density map of the OCTA. For each MvD, a line was drawn to equally bisect the angular circumferential margins of the MvD from the ONH center, as previously reported,<sup>29</sup> to define the location of the MvD. Disagreements between the 2 observers in assessing presence and location of MvD were adjudicated by the third experienced grader (SM). The location of MvDs was categorized as hemispheric (superior, inferior, or both) corresponding to those on OCT-A and OCT parameters.

### Statistical analysis

Patient and eye characteristics data were presented as mean (95% confidence interval (CI)) for continuous variables and count (%) for categorical variables. Interobserver agreement in detecting presence of MvD was assessed using kappa statistics (i.e., kappa value) and interclass correlation coefficient (ICC) was used for MvD area and angular circumference measurements. Categorical variables were compared using the chi-square test.

Mixed-effects modeling was used to compare ocular parameters among groups. A joint longitudinal linear mixed effects model was used to estimate the rates of change for both cpRNFL and MvD, with random effects applied at the eye level. The details on the use of these models for evaluation of rates of change in glaucoma and to model longitudinal processes have been published.<sup>30,31</sup> Briefly, linear mixed models estimate the average rate of change in an outcome variable using a linear function of time, and subject- and eye-specific deviations from this average rate are introduced by random slopes, while taking into account for the potential influence of inter-eye correlation. In joint longitudinal modeling, both cpRNFL and MvD data are modeled simultaneously. This allows a better determination of the true underlying relationship between the two outcomes by considering measurement error. Specifically, we evaluated the association between cpRNFL rate of change with 1) MvD area and 2) MvD angular circumference rate of change.

The effect of rates of MvD area or angular circumference changes as well as potential predictors, such as age, mean IOP during follow-up and any other variable in which the P value was <0.1 in univariable analysis on the RNFL thinning during the follow-up was introduced in the multivariable model. Statistical analyses were performed using Stata version 16.0 (StataCorp, College Station, TX). P values of less than 0.05 were considered statistically significant for all analyses.

## RESULTS

A total of 101 eyes of 75 POAG patients were initially included. Among them, 10 eyes of 7 patients were excluded due to the presence of artifacts or shadowing from large vessels, resulting in 91 eyes of 68 patients that were finally included in the analysis.

The demographic characteristics are provided in Table 1. Mean (95%CI) age was 69.0 (66.6, 71.4) years, and mean (95% CI) baseline VF MD was  $-4.7$  ( $-5.8$ ,  $-3.6$ ) dB. The mean (95%CI) number of OCT and OCTA visits were 6.2 (5.8, 6.6), and 5.7 (5.4, 6.0), over a mean follow-up of 4.0 (3.9, 4.2) years. Interobserver agreement in detecting the presence of MvD (95%CI) was excellent ( $k=0.988$  (0.986, 0.990)). The ICC for interobserver reproducibility in measuring the area and the angular circumference of MvD (95%CI) was 0.977 (0.973, 0.980) and 0.977 (0.973, 0.980), respectively.

Peripapillary MvD was detected in 53 (58.2%) eyes at baseline, whereas 17 (18.6%) eyes that did not show MvD at baseline developed it over the follow-up period. Among the 53 eyes having MvD at baseline, in 21 eyes (39.6%) it was located in the inferior hemisphere, 4 eyes (7.6%) in the superior hemisphere, and in 28 eyes (52.8%) MvD was present in both hemispheres.

The mean (95%CI) MvD area was 0.15 (0.09, 0.22)  $\text{mm}^2$  at baseline and 0.32  $\text{mm}^2$  (0.24, 0.41) at final follow-up ( $P < 0.001$ ). The mean (95%CI) MvD angular circumference was  $41.3^\circ$  (29.3, 53.4) at the baseline, while it was  $85.4^\circ$  (69.4, 101.4) at the final follow-up ( $P < 0.001$ ). The mean (95%CI) rates of change of MvD area and angular circumference were 0.05 (0.04, 0.06)  $\text{mm}^2/\text{year}$ , and 13.22 (10.67, 15.76) degree/year, respectively. The rates of change of MvD area in eyes with mean IOP during follow-up  $>16$  mmHg were significantly lower compared to those with mean IOP during follow-up IOP  $<16$  mmHg (0.02 [ $-0.03$ , 0.00]  $\text{mm}^2/\text{year}$  lower,  $P=0.049$ ).

Figure 1 shows a representative case of the relationship between MvD area enlargement and cpRNFL thinning in a glaucomatous patient.

Table 2 shows the effect of corrected MvD area change on cpRNFL thinning in univariable and multivariable mixed model. In univariable analysis, rate of change of MvD area was significantly associated with cpRNFL thinning ( $-6.11$  [ $-12.60$ , 0.38]  $\mu\text{m}/\text{year}$  per 1  $\text{mm}^2/\text{year}$  increase;  $P=0.064$ ). After adjustment for confounding factors (i.e., age, self-reported hypertension and mean IOP during follow-up), the rate of change of MvD area and baseline VF MD (coefficient [95%CI] were significantly associated with cpRNFL progression ( $-8.80$  [ $-15.24$ ,  $-2.36$ ]  $\mu\text{m}/\text{year}$  per 1  $\text{mm}^2/\text{year}$  increase;  $P=0.008$ , and 0.06 [0.03, 0.09] dB/year per 1 dB worse;  $P < 0.001$ ).

In eyes with MvD in the inferior hemisphere at baseline ( $n=21$ ), the RNFL thinning tended to be faster in the inferior hemisphere ( $-0.48$  ( $-0.84$ ,  $-0.13$ )  $\mu\text{m}/\text{year}$ ) compared to the superior hemisphere ( $-0.37$  ( $-0.63$ ,  $-0.12$ )  $\mu\text{m}/\text{year}$ ), although this difference was not significant ( $P=0.609$ ).

Table 3 shows the effect of MvD angular circumference on cpRNFL progression in univariate and multivariate mixed models. In univariable analysis, the rate of change of MvD angular circumference (coefficient [95%CI]:  $-0.26$  [0.49,  $-0.04$ ]  $\mu\text{m}/\text{year}$  per 10 degree/year;  $P = 0.021$ ), baseline VF MD (coefficient [95%CI]: 0.03 [0.01, 0.05]  $\mu\text{m}/\text{year}$  per 1 dB worse;  $P = 0.002$ ) and self-reported hypertension (coefficient [95%CI]: 0.30 [ $-0.01$ , 0.65]  $\mu\text{m}/\text{year}$ ;  $P=0.098$ ) were found to be associated with MvD angular circumference enlargement. After adjustment for confounding factors, MvD angular circumference rate of

change (coefficient [95% CI]:  $-0.30$  [ $-0.53, -0.08$ ]  $\mu\text{m}/\text{year}$  per 10 degree/year;  $P = 0.009$ ) and baseline VF MD (coefficient [95% CI]:  $0.05$  [ $0.02, 0.07$ ];  $P < 0.001$ ), were the main factors associated with cpRNFL thinning.

While MvD area change was associated with RNFL thinning in early ( $> -6\text{dB}$ ) glaucoma eyes (coefficient (95% CI):  $-12.01$  ( $-21.84, -2.18$ )  $1 \text{ mm}^2/\text{year}$  per  $1 \mu\text{m}/\text{year}$ ,  $P = 0.018$ ) in univariable analysis, no association was observed between MvD area change and RNFL thinning in moderate-advanced ( $< -6\text{dB}$ ) glaucoma eyes (coefficient (95% CI):  $-5.57$  ( $-14.31, 3.18$ ),  $P = 0.198$ ).

## DISCUSSION

With more than four years of follow-up, this study demonstrated that more than two-thirds of POAG eyes showed evidence of MvD throughout the follow-up. We also showed that faster rates of progressive cpRNFL thinning were associated faster increases in MvD area and circumference ( $R^2$  ranged from 0.10 to 0.30), and may be useful for assessing progression in glaucomatous patients. These findings enhanced the current understanding of the role of MvD in glaucoma pathogenesis and may provide an additional strategy for monitoring glaucoma using OCT-A technology.

Previous studies reported a significant association between MvD and parameters of functional and structural damage, such as VF,<sup>6,21</sup> cpRNFL,<sup>6,32</sup> and GCC.<sup>33</sup> The presence of MvD at baseline was more frequently found in patients with ocular and systemic prognostic factors and it appeared one of the strongest predictors of accelerated progression.<sup>34</sup> Recently, studies reported an enlargement of MvD in some patients with glaucoma;<sup>12,29</sup> this suggests that the extent of the enlargement might be related to the rate of visual loss. In the present study, the rates of change of MvD were significantly associated with the rates of cpRNFL thinning throughout a mean of 5.7 OCT-A visits and 4 years of follow-up. In separate models, both MvD area and angular circumference changes appeared to be independently associated with concurrent cpRNFL thinning. Moreover, this association was higher in the early stages of glaucoma compared to the moderate-advanced stages. In agreement with our findings, Kim et al. showed faster global cpRNFL thinning in eyes with larger increases in MvD area at 2 years follow-up visit.<sup>12</sup> Similarly, Lee et al. observed faster rates of VF loss in eyes with greater angular enlargement of MvD whereas the VF progression was slower in eyes with stable or little MvD angular enlargement.<sup>29</sup> However none of the previous studies estimated the trend of changes of MvD area and angular circumference; they evaluated the MvD only twice, once at the beginning and once at the final visit. We demonstrated that the assessment of MvD trend using OCT-A may represent an adjunctive parameter that can help clinicians to identify and monitor progressive glaucomatous damage.

In eyes with MvD in inferior hemisphere at baseline, RNFL thinning tended to be faster in the inferior hemisphere compared to superior hemisphere. A relatively small sample size does not have the power to expose such a small effect, possibly resulting in a type II error. Further larger studies are needed to assess the topographical association between MvD location and RNFL thinning.

Previously, Leung CK et al. reported that widening of RNFL, detected by Cirrus SD-OCT, was the predominant pattern of progressive change of RNFL defects.<sup>35</sup> Although the present study examined the relationship between MvD changes and RNFL thinning, further studies are needed to elucidate the topographic correlation between the location of MvD and the location of RNFL widening using other OCT instruments.

As MvD mostly constitutes a localized perfusion defect of the choriocapillaris and choroidal microvasculature in the  $\beta$ -PPA region, it may indicate an impaired perfusion of the ONH deep tissues. Since vascular factors may play a relevant role in the prognosis of OAG,<sup>36,37</sup> the presence of MvD and its changes may be considered a parameter that represents accelerated glaucomatous damage. In the present study more than two-thirds of POAG eyes showed evidence of MvD at baseline or over the follow-up. Although it is still unclear whether MvD is primary or secondary to RNFL loss, there are several hypotheses to explain this relationship. One possible explanation is that MvD changes may be involved in a pathophysiological process that leads to glaucoma progression. As MvD is associated with risk factors closely linked to vascular insufficiency at the ONH, eyes with signs of increasing hypoperfusion to the ONH, such as an enlargement of the MvD, may show faster progression compared to those without MvD changes. Another hypothesis is that MvD may be the result of a secondary change associated with progressive RNFL damage. A diminished metabolic need related to progressive retinal ganglion cell loss may be associated with reduced or unstable perfusion in the deep-layer ONH structures, resulting in the enlargement of MvD.

Interestingly, in the present study, the rates of change of MvD area in eyes with mean IOP during follow-up  $>16$  mmHg were significantly lower compared to those with mean IOP during follow-up IOP  $<16$  mmHg. These findings suggest that changes in MvD size are not correlated with IOP, confirming that IOP-independent mechanisms, such as an insufficient or unstable perfusion, have a role in the process that leads to MvD changes.<sup>38</sup> Alternatively, it may be related to the high probably of aggressive treatment in eyes with faster RNFL thinning – which may result in lower IOP associated with not only faster RNFL thinning, but also greater MvD changes. In addition, no significant association was found between average IOP during follow-up and the rates of RNFL thinning in eyes with MvD. These findings differ from the study by Kim et al.<sup>12</sup>, who found that IOP during follow-up was an independent parameter for RNFL thinning in eyes with MvD.

This study has several limitations. First, MvD size was measured on the en-face choroidal vessel density map, which subject to many limitations. To minimize subjectivity in the measurements of MvD, we defined MvD as a complete loss of the choroidal microvasculature with a size of 200 microns or greater in diameter, a method that has been validated in previous studies.<sup>6</sup> In addition, large overlying vessels or DHs may project onto en-face choroidal vessel density images, and may induce projection artifacts or shadows or make it difficult to detect or define MvD boundaries. In order to reduce these potential false negatives, MvD was defined by 2 examiners using both en-face and B-scan images and we found a good interobserver agreement ( $k=0.977$ ) between graders. Second, MvD area and angular circumference were measured on en-face images using the automatic demarcation of the BMO, and this was not accurately demarcated in some eyes. To overcome this limitation,

disc margin errors were manually corrected before the quantitative analysis of MvD by a trained observer, who was masked to the clinical characteristics of the subjects. Third, the en-face choroidal vessel density image was used to detect MvD. Although this slab includes both choroid and inner sclera, the choroid is not segmented specifically and one cannot assume that it represents only the choroidal layer. Fourth, in our analysis we evaluated the association of the rate of global RNFL thinning with MvD area and circumference which are by definition focal measurements. It is possible that stronger associations would be found if sectoral RNFL thinning was included in the models. The Spectralis was used to evaluate cpRNFL thinning since its reproducibility of cpRNFL is better than with Optovue.<sup>39,40</sup> Avanti does not have protocol for disc-fovea alignment and the optic nerve head sectors might not be completely correspond between the two instruments. However, the detailed topographic correlation between the change in MvD area and angle circumference and the angular location of progressive cpRNFL loss was not evaluated in the present study. Thus, our results are minimally affected by this issue.

Last, ocular magnification effects associated with axial length might have influenced MvD area as measured by OCT-A. However, eyes with axial length > 27 mm were excluded in the current study. Moreover, Littmann's formula was used to correct the magnification effect.

In conclusion, faster change in MvD area and angle circumference was moderately, and significantly, associated with faster cpRNFL thinning in glaucoma eyes during a mean follow-up of 4 years. Future studies are needed to assess whether MvD enlargement can improve monitoring of glaucoma patients.

## ACKNOWLEDGEMENTS/FUNDING

National Institutes of Health/National Eye Institute Grants R01EY029058, R01EY011008, R01EY026574, R01EY019869 and R01EY027510; Core Grant P30EY022589; by the donors of the National Glaucoma Research Program (no grant number), a program of the BrightFocus Foundation grant (G2017122), an unrestricted grant from Research to Prevent Blindness (New York, NY); UC Tobacco Related Disease Research Program (T31IP1511); and grants for participants' glaucoma medications from Alcon, Allergan, Pfizer, Merck, and Santen. The sponsor or funding organizations had no role in the design or conduct of this research.

## FINANCIAL DISCLOSURES

Eleonora Micheletti: none; Sasan Moghimi: none; Takashi Nishida: none; Nevin W. El-Nimri: none; Golnoush Mahmoudinezhad: none; Alireza Kamalipour: none; Harsha L. Rao: none; Linda M. Zangwill: National Eye Institute (F), Carl Zeiss Meditec Inc. (F), Heidelberg Engineering GmbH (F), OptoVue Inc. (F, R), Topcon Medical Systems Inc. (F, R) Merck (C); Robert N. Weinreb: Aerie Pharmaceuticals (C), Alcon (C), Allergan (C), Bausch & Lomb (C), Eyenovia (C), Novartis (C), Unity (C), Heidelberg Engineering (F), Carl Zeiss Meditec (F), Genentech (F), Konan (F), OptoVue (F), Topcon (F), Optos (F), Centervue (F).

## REFERENCES

1. Weinreb RN, Khaw PT. Primary open-angle glaucoma. *Lancet*. 2004;363(9422):1711–1720. [PubMed: 15158634]
2. Weinreb RN, Aung T, Medeiros FA. The pathophysiology and treatment of glaucoma: a review. *JAMA*. 2014;311(18):1901–1911. [PubMed: 24825645]
3. Yarmohammadi A, Zangwill LM, Diniz-Filho A, et al. Optical Coherence Tomography Angiography Vessel Density in Healthy, Glaucoma Suspect, and Glaucoma Eyes. *Invest Ophthalmol Vis Sci*. 2016;57(9):OCT451–459. [PubMed: 27409505]

4. Mansouri K Optical coherence tomography angiography and glaucoma: searching for the missing link. *Expert Rev Med Devices*. 2016;13(10):879–880. [PubMed: 27580072]
5. Lee EJ, Lee KM, Lee SH, Kim TW. Parapapillary Choroidal Microvasculature Dropout in Glaucoma: A Comparison between Optical Coherence Tomography Angiography and Indocyanine Green Angiography. *Ophthalmology*. 2017;124(8):1209–1217. [PubMed: 28433445]
6. Suh MH, Zangwill LM, Manalastas PI, et al. Deep Retinal Layer Microvasculature Dropout Detected by the Optical Coherence Tomography Angiography in Glaucoma. *Ophthalmology*. 2016;123(12):2509–2518. [PubMed: 27769587]
7. Jo YH, Kwon J, Jeong D, Shon K, Kook MS. Rapid Central Visual Field Progression Rate in Eyes with Open-Angle Glaucoma and Choroidal Microvasculature Dropout. *Sci Rep*. 2019;9(1):8525. [PubMed: 31189960]
8. Kwon JM, Weinreb RN, Zangwill LM, Suh MH. Parapapillary Deep-Layer Microvasculature Dropout and Visual Field Progression in Glaucoma. *Am J Ophthalmol*. 2019;200:65–75. [PubMed: 30578786]
9. Kwon JM, Weinreb RN, Zangwill LM, Suh MH. Juxtapapillary Deep-Layer Microvasculature Dropout and Retinal Nerve Fiber Layer Thinning in Glaucoma. *Am J Ophthalmol*. 2021;227:154–165. [PubMed: 33631124]
10. Lee SH, Lee EJ, Kim TW. Topographic correlation between juxtapapillary choroidal thickness and parapapillary deep-layer microvasculature dropout in primary open-angle glaucoma. *Br J Ophthalmol*. 2018;102(8):1134–1140. [PubMed: 29101122]
11. Lee EJ, Kim JA, Kim TW. Influence of Choroidal Microvasculature Dropout on the Rate of Glaucomatous Progression: A Prospective Study. *Ophthalmol Glaucoma*. 2020;3(1):25–31. [PubMed: 32672639]
12. Kim JA, Lee EJ, Kim TW. Evaluation of Parapapillary Choroidal Microvasculature Dropout and Progressive Retinal Nerve Fiber Layer Thinning in Patients With Glaucoma. *JAMA Ophthalmol*. 2019;137(7):810–816. [PubMed: 31120486]
13. Park HL, Kim JW, Park CK. Choroidal Microvasculature Dropout Is Associated with Progressive Retinal Nerve Fiber Layer Thinning in Glaucoma with Disc Hemorrhage. *Ophthalmology*. 2018;125(7):1003–1013. [PubMed: 29486903]
14. Rao HL, Sreenivasaiah S, Dixit S, et al. Choroidal Microvascular Dropout in Primary Open-angle Glaucoma Eyes With Disc Hemorrhage. *J Glaucoma*. 2019;28(3):181–187. [PubMed: 30601223]
15. Lee K, Bae HW, Lee SY, Seong GJ, Kim CY. Hierarchical Cluster Analysis of Peripapillary Retinal Nerve Fiber Layer Damage and Macular Ganglion Cell Loss in Open Angle Glaucoma. *Korean J Ophthalmol*. 2020;34(1):56–66. [PubMed: 32037750]
16. Kim GN, Lee EJ, Kim TW. Parapapillary choroidal microvasculature dropout in nonglaucomatous healthy eyes. *Acta Ophthalmol*. 2020;98(6):e754–e760. [PubMed: 32115892]
17. Suh MH, Na JH, Zangwill LM, Weinreb RN. Deep-layer Microvasculature Dropout in Preperimetric Glaucoma Patients. *J Glaucoma*. 2020;29(6):423–428. [PubMed: 32205833]
18. Han JC, Choi JH, Park DY, Lee EJ, Kee C. Border Tissue Morphology Is Spatially Associated with Focal Lamina Cribrosa Defect and Deep-Layer Microvasculature Dropout in Open-Angle Glaucoma. *Am J Ophthalmol*. 2019;203:89–102. [PubMed: 30825418]
19. Lee SH, Kim TW, Lee EJ, Girard MJA, Mari JM. Focal lamina cribrosa defects are not associated with steep lamina cribrosa curvature but with choroidal microvascular dropout. *Sci Rep*. 2020;10(1):6761. [PubMed: 32317767]
20. Park SC, De Moraes CG, Teng CC, Tello C, Liebmann JM, Ritch R. Initial parafoveal versus peripheral scotomas in glaucoma: risk factors and visual field characteristics. *Ophthalmology*. 2011;118(9):1782–1789. [PubMed: 21665283]
21. Lee EJ, Kim TW, Kim JA, Kim JA. Central Visual Field Damage and Parapapillary Choroidal Microvasculature Dropout in Primary Open-Angle Glaucoma. *Ophthalmology*. 2018;125(4):588–596. [PubMed: 29224927]
22. Abe RY, Diniz-Filho A, Costa VP, Gracitelli CP, Baig S, Medeiros FA. The Impact of Location of Progressive Visual Field Loss on Longitudinal Changes in Quality of Life of Patients with Glaucoma. *Ophthalmology*. 2016;123(3):552–557. [PubMed: 26704883]

23. Sample PA, Girkin CA, Zangwill LM, et al. The African Descent and Glaucoma Evaluation Study (ADAGES): design and baseline data. *Arch Ophthalmol.* 2009;127(9):1136–1145. [PubMed: 19752422]
24. Girkin CA, Sample PA, Liebmann JM, et al. African Descent and Glaucoma Evaluation Study (ADAGES): II. Ancestry differences in optic disc, retinal nerve fiber layer, and macular structure in healthy subjects. *Arch Ophthalmol.* 2010;128(5):541–550. [PubMed: 20457974]
25. Wu H, de Boer JF, Chen TC. Reproducibility of retinal nerve fiber layer thickness measurements using spectral domain optical coherence tomography. *J Glaucoma.* 2011;20(8):470–476. [PubMed: 20852437]
26. Zang P, Gao SS, Hwang TS, et al. Automated boundary detection of the optic disc and layer segmentation of the peripapillary retina in volumetric structural and angiographic optical coherence tomography. *Biomed Opt Express.* 2017;8(3):1306–1318. [PubMed: 28663830]
27. Aykut V, Oner V, Tas M, Iscan Y, Agachan A. Influence of axial length on peripapillary retinal nerve fiber layer thickness in children: a study by RTVue spectral-domain optical coherence tomography. *Curr Eye Res.* 2013;38(12):1241–1247. [PubMed: 23972028]
28. Bennett AG, Rudnicka AR, Edgar DF. Improvements on Littmann's method of determining the size of retinal features by fundus photography. *Graefes Arch Clin Exp Ophthalmol.* 1994;32(6):361–367. [PubMed: 8082844]
29. Lee JY, Shin JW, Song MK, Hong JW, Kook MS. An Increased Choroidal Microvasculature Dropout Size is Associated With Progressive Visual Field Loss in Open-Angle Glaucoma. *Am J Ophthalmol.* 2021;223:205–219. [PubMed: 33129811]
30. Crowther MJ, Lambert PC, Abrams KR. Adjusting for measurement error in baseline prognostic biomarkers included in a time-to-event analysis: a joint modelling approach. *BMC Med Res Methodol.* 2013;13:146. [PubMed: 24289257]
31. Medeiros FA, Zangwill LM, Alencar LM, Sample PA, Weinreb RN. Rates of progressive retinal nerve fiber layer loss in glaucoma measured by scanning laser polarimetry. *Am J Ophthalmol.* 2010;149(6):908–915. [PubMed: 20378095]
32. Lin S, Cheng H, Zhang S, et al. Parapapillary Choroidal Microvasculature Dropout Is Associated With the Decrease in Retinal Nerve Fiber Layer Thickness: A Prospective Study. *Invest Ophthalmol Vis Sci.* 2019;60(2):838–842. [PubMed: 30811547]
33. Micheletti E, Moghimi S, El-Nimri N, et al. Relationship of macular ganglion cell complex thickness to choroidal microvasculature drop-out in primary open-angle glaucoma. *Br J Ophthalmol.* 2022;2022 Jan 13:bjophthalmol-2021–320621.
34. Lee EJ, Kim TW, Kim JA, et al. Elucidation of the Strongest Factors Influencing Rapid Retinal Nerve Fiber Layer Thinning in Glaucoma. *Invest Ophthalmol Vis Sci.* 2019;60(10):3343–3351. [PubMed: 31370062]
35. Leung CK, Yu M, Weinreb RN, Lai G, Xu G, Lam DS. Retinal nerve fiber layer imaging with spectral-domain optical coherence tomography: patterns of retinal nerve fiber layer progression. *Ophthalmology.* 2012;119(9):1858–1866. [PubMed: 22677426]
36. Flammer J, Orgul S, Costa VP, et al. The impact of ocular blood flow in glaucoma. *Prog Retin Eye Res.* 2002;21(4):359–393. [PubMed: 12150988]
37. Weinreb RN. Ocular blood flow in glaucoma. *Can J Ophthalmol.* 2008;43(3):281–283. [PubMed: 18504463]
38. Rao HL, Sreenivasaiah S, Riyazuddin M, et al. Choroidal microvascular dropout in primary angle closure glaucoma. *American journal of ophthalmology.* 2019;199:184–192. [PubMed: 30552893]
39. Pierro L, Gagliardi M, Iuliano L, Ambrosi A, Bandello F. Retinal nerve fiber layer thickness reproducibility using seven different OCT instruments. *Invest Ophthalmol Vis Sci.* 2012;53(9):5912–5920. [PubMed: 22871835]
40. Nishida T, Moghimi S, Hou H, et al. Long-term reproducibility of optical coherence tomography angiography in healthy and stable glaucomatous eyes. *Br J Ophthalmol.* 2021;Dec 21:2021–320034.

### Synopsis

In this observational cohort study, the rates of choroidal microvasculature dropout area and angular circumference change over time were associated with concurrent rates of circumpapillary retinal nerve fiber loss in glaucomatous eyes.

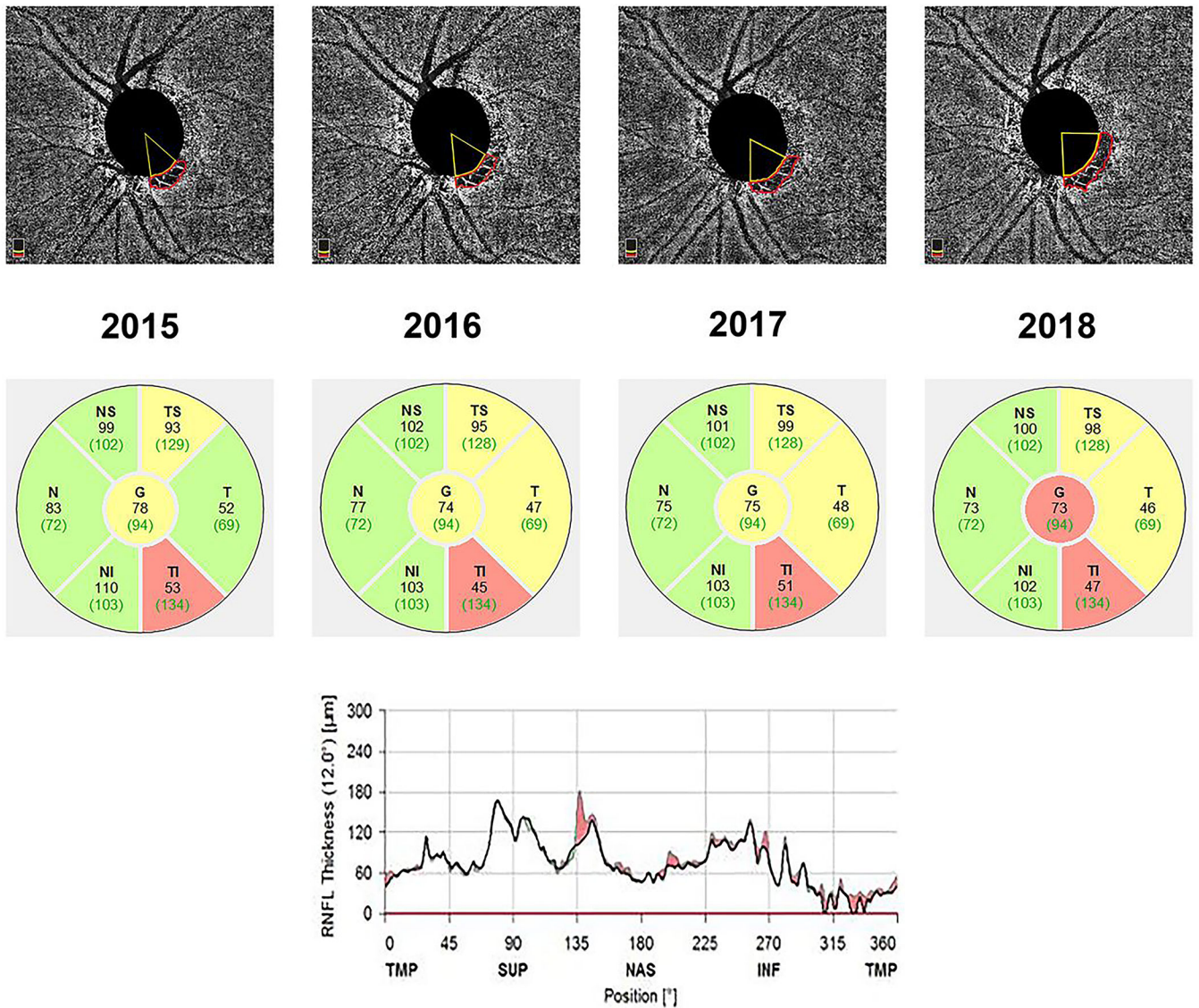


**Figure 1.** En-face choroidal VD map showing MvD area changes and corresponding RNFL thinning over 4-year follow-up in a POAG eye. The rate of MvD area (red outline) and angular circumference (yellow outline) enlargement was 0.04 mm<sup>2</sup>/year and 8.40 degree/year, respectively. The rate of global RNFL thinning was -0.50 µm/year

**Table 1.**

## Demographics and Clinical characteristics of the subjects

<b>Variables</b>	
Patients (eyes)	68 patients (91 eyes)
Baseline age (years)	69.0 (66.6, 71.4)
Gender (Female/ Male)	34/34
Race (African American/Non-African American)	19/49
Self-reported hypertension, n (%)	46 (66.7)
Self-reported diabetes, n (%)	11 (15.9)
Axial length (mm)	24.1 (23.9, 24.4)
CCT ( $\mu\text{m}$ )	532.7 (523.3, 542.1)
Baseline IOP (mmHg)	14.1 (13.2, 14.9)
Disease Severity by baseline 24–2 VF MD	
Early glaucoma (MD $-6$ dB), Eye No. (%)	67 (73.6)
Moderate and advanced glaucoma (MD $<-6$ dB), Eye No. (%)	24 (26.4)
Baseline VF MD (dB)	$-4.7$ ( $-5.8$ , $-3.6$ )
cpRNFL at baseline ( $\mu\text{m}$ )	72.5 (69.3, 75.7)
cpRNFL at the last visit ( $\mu\text{m}$ )	70.0 (66.9, 73.2)
Corrected MvD area at baseline ( $\text{mm}^2$ )	0.15 (0.09, 0.22)
Corrected MvD area at the last visit ( $\text{mm}^2$ )	0.32 (0.24, 0.40)
MvD angle at baseline (degree)	41.3 (29.3, 53.4)
MvD angle at the last visit (degree)	85.4 (69.4, 101.4)
OCT follow-up visits (n)	6.2 (5.8, 6.6)
OCTA follow-up visits (n)	5.7 (5.5, 6.0)
Follow-up (years)	4.0 (3.9, 4.2)

CCT = central corneal thickness; cpRNFL = circumpapillary retinal nerve fiber layer; IOP = intraocular pressure; MD = mean deviation; MvD = microvascular dropout; n = number; OCT = optical coherence tomography; OCTA = optical coherence tomography angiography; VF = visual field. Values are shown in mean (95% confidence interval), unless otherwise indicated.

**Table 2.**

Association between rate of cpRNFL Thinning Over Time and Factors including MvD Area (n= 91 eyes)

Variables	Univariable Model		Multivariable Model 1		Multivariable Model 2	
	$\beta$ , 95 % CI	P value	$\beta$ , 95 % CI	P value	$\beta$ , 95 % CI	P value
Age, per 10 years older	0.04 (-0.13, 0.22)	0.639	0.10 (-0.04, 0.25)	0.164	0.01 (-0.01, 0.02)	0.239
Gender: Female	0.20 (-0.12, 0.51)	0.217				
Race: African American	-0.06 (-0.43, 0.31)	0.747				
Self-reported hypertension	0.27 (-0.10, 0.64)	0.154				
Self-reported diabetes	0.17 (-0.25, 0.59)	0.430				
Axial length, per 1mm longer	0.05 (-0.05, 0.15)	0.323				
CCT, per 100 $\mu$ m thinner	-0.01 (-0.29, 0.28)	0.961				
Baseline IOP, per 1 mmHg higher	-0.02 (-0.05, 0.01)	0.252	0.00 (-0.03, 0.03)	0.933		
Mean IOP during follow-up, per 1 mmHg higher	-0.02 (-0.05, 0.02)	0.312			-0.01 (-0.04, 0.02)	0.538
Baseline VF MD, per 1 dB worse	0.04 (0.01, 0.06)	<b>0.002</b>	0.01 (-0.01, 0.04)	0.301	0.06 (0.03, 0.09)	<b>&lt;0.001</b>
Scan Quality, per 1 higher	-0.13 (-0.30, 0.04)	0.138				
Follow-up period, per 1 year longer	-0.03 (-0.22, 0.15)	0.739				
No. of OCT follow-up visits	0.04 (-0.04, 0.13)	0.305				
MvD area at baseline, per 1 mm <sup>2</sup>	0.81 (0.49, 1.13)	<b>&lt;0.001</b>	0.76 (0.21, 1.32)	<b>0.008</b>		
MvD area change, per 1 mm <sup>2</sup> /year	-6.11 (-12.60, 0.38)	<b>0.064</b>			-8.80 (-15.24, -2.36)	<b>0.008</b>

CCT = central corneal thickness; IOP = intraocular pressure; MD = mean deviation; MvD = microvascular dropout; OCT = optical coherence tomography; VF = visual field. Values are shown in  $\beta$  coefficient (95% confidence interval). Statistically significant P values are shown in bold. The value of MvD area was multiplied by one hundred to enhance the readability of the Table.

**Table 3.**

Association between rate of cpRNFL Thinning Over Time and Factors including MvD angular circumference (n= 91 eyes)

Variables	Univariable Model		Multivariable Model 1		Multivariable Model 2	
	$\beta$ , 95 % CI	P value	$\beta$ , 95 % CI	P value	$\beta$ , 95 % CI	P value
Age, per 10 years older	0.06 (-0.10, 0.22)	0.443	0.05 (-0.10, 0.19)	0.512	0.08 (-0.05, 0.21)	0.201
Gender: Female	0.21 (-0.09, 0.51)	0.173				
Race: African American	-0.02 (-0.37, 0.33)	0.908				
Self-reported hypertension	0.30 (-0.06, 0.65)	<b>0.098</b>	0.29 (-0.08, 0.65)	0.123	0.15 (-0.13, 0.43)	0.297
Self-reported diabetes	0.15 (-0.27, 0.58)	0.471				
Axial length, per 1mm longer	0.05 (-0.05, 0.16)	0.322				
CCT, per 100 $\mu$ m thinner	0.01 (-0.26, 0.29)	0.916				
Baseline IOP, per 1 mmHg higher	-0.01 (-0.04, 0.01)	0.294	-0.01 (-0.03, 0.02)	0.702		
Mean IOP during follow-up, per 1 mmHg higher	-0.01 (-0.04, 0.02)	0.360			-0.01 (-0.03, 0.02)	0.610
Baseline VF MD, per 1 dB worse	0.03 (0.01, 0.05)	<b>0.002</b>	0.02 (-0.01, 0.05)	0.121	0.05 (0.02, 0.07)	<b>&lt;0.001</b>
Scan Quality, per 1 higher	-0.14 (-0.31, 0.03)	0.112				
Follow-up period, per 1 year longer	-0.02 (-0.20, 0.16)	0.856				
No. of OCT follow-up visits	0.05 (-0.03, 0.13)	0.215				
MvD angle at baseline, per 1 degree	0.03 (0.01, 0.05)	<b>0.007</b>	0.02 (-0.01, 0.05)	0.160		
MvD angle change, per 10 degrees wider/year	-0.26 (-0.49, -0.04)	<b>0.021</b>			-0.30 (-0.53, -0.08)	<b>0.009</b>

CCT = central corneal thickness; IOP = intraocular pressure; MD = mean deviation; MvD = microvascular dropout; OCT = optical coherence tomography; VF = visual field. Values are shown in  $\beta$  coefficient (95% confidence interval). Statistically significant P values are shown in bold.